Dye Aggregates in Water

DOI: 10.1002/anie.201308963

Hierarchical Growth of Fluorescent Dye Aggregates in Water by Fusion of Segmented Nanostructures**

*Xin Zhang, Daniel Görl, Vladimir Stepanenko, and Frank Würthner**

Abstract: *Dye aggregates are becoming increasingly attractive for diverse applications, in particular as organic electronic and sensor materials. However, the growth processes of such aggregates from molecular to small assemblies up to nanostructures is still not properly understood, limiting the design of materials' functional properties. Here we elucidate the supramolecular growth process for an outstanding class of functional dyes, perylene bisimides (PBIs), by transmission electron microscopy (TEM), cryogenic scanning electron microscopy (cryo-SEM), and atomic force microscopy (AFM). Our studies reveal a sequential growth of amphiphilic PBI dyes from nanorods into nanoribbons in water by fusion and fission processes. More intriguingly, the fluorescence observed for higher hierarchical order nanoribbons was enhanced relative to that of nanorods. Our results provide insight into the relationship between molecular, morphological, and functional properties of self-assembled organic materials.*

Molecular hierarchical organization is essential in natural processes and regulates the self-assembly of small molecules into a rich variety of functional high-order nanostructures with precise molecular arrangements such as DNA, pore-forming proteins, G-quadruplex, and even microorganisms such as tobacco mosaic virus.[1–3] These natural nanostructures can be replicated and delivered in biological systems by lipid fusion and fission processes that are accomplished by self-assembled natural amphiphilic molecules.[4] The miraculous bottom-up self-assembly of natural amphiphiles from small compartments to the formation of tissues inspires chemists to create new functional, molecularly precise nanostructures in water.[5–7]

In the last decade, significant progress has been achieved and a multitude of fascinating architectures formed by the self-assembly of nonconventional amphiphiles in aqueous media have been reported,[8,9] including micelles and bilayer vesicles,[10,11] fibers,[12,13] nanotubes,[14,15] nanotoroids, and nanorings.[16] In general, however, these studies focused on the structures of the final products and not on their formation. To shed light on the latter, amphiphilic perylene bisimide (PBI) dyes[17,18] appear to be the best suited because they exhibit the largest intermolecular interaction energies of all dyes,[19] which is further enhanced in water by a pronounced hydrophobic effect.[20] For this reason, PBI aggregates in water are quite robust[19,20] and this raised our expectation to achieve long-range structural order beyond that achieved for other smaller and more flexible amphiphilic π-scaffolds which are packed together by weaker noncovalent interactions. Here, we elucidate the growth process for PBI **1** (Figure 1) from a single-component system to small molecular assemblies up to large nanostructures by transmission electron microscopy (TEM) with resolution on the molecular level. Remarkably, and this observation is unprecedented to the best of our knowledge, the fluorescence properties of these dye aggregates were enhanced for the higher hierarchical order nanostructures.

The molecular structure of PBI **1** consists of a hydrophobic perylene core (shown in orange in Figure 1 a) with hydrophilic oligoethylene glycol (OEG) chains on both ends (shown in blue). Dissolved PBI **1** shows green fluorescence (Figure 1 b) in dilute (2.0×10^{-6} M) THF solution. When the solvent is gradually changed from THF to water, even at this low concentration a complete transformation from monomers into aggregates is observed (Figure 1 c). Based on our earlier work on the self-assembly of structurally related PBI dyes in organic solvents,[20] we attribute the UV/Vis spectra at low THF content and in pure water (see Figure S9 in the Supporting Information) to 1D columnar π-stacks of rotationally displaced PBI molecules. Since the binding constant for PBI–PBI stacking in water is considerably higher than that in THF,[20] however, even in very dilute solutions more than 99 % of the molecules are aggregated in extended π-stacks.[22]

As a consequence of the strong PBI–PBI stacking in water, already at a slightly higher concentration (0.077 mg mL^{-1}; ca. 0.05 mM), PBI **1** self-assembles into well-defined nanorods, as observed by transmission electron microscopy (TEM) (Figure 2 a). These nanorods have a uniform diameter of 4 nm, which corresponds to the length of one molecule. Interestingly, a segmented structure within these nanorods was further observed by TEM (Figure 2 a, inset). To the best of our knowledge, such highly resolved TEM images with precision at the molecular level has not been achieved so far for organic dye aggregates. We attribute this unusually high resolution to the preferential positive staining of the carbonyl and hydrophilic glycol chains of the PBI dyes.[23] These molecular-level-resolved TEM images give direct evidence that the planar PBI **1** self-assembles in a very regular manner into a helically wound columnar π-stack by cofacial intermolecular π–π stacking interactions (Figure 2 c). Analysis of the cross-section electron density (relative darkness) along these nanorods revealed an average distance of

[*] Dr. X. Zhang, D. Görl, Dr. V. Stepanenko, Prof. Dr. F. Würthner
Universität Würzburg, Center for Nanosystems Chemistry
and Institut für Organische Chemie
Am Hubland, 97074 Würzburg (Germany)
E-mail: wuerthner@chemie.uni-wuerzburg.de

[**] We thank the DFG (grant no. Wu 317/11) for financial support and Prof. Georg Krohne for his help with the TEM measurements.

Supporting information for this article is available on the WWW under http://dx.doi.org/10.1002/anie.201308963.

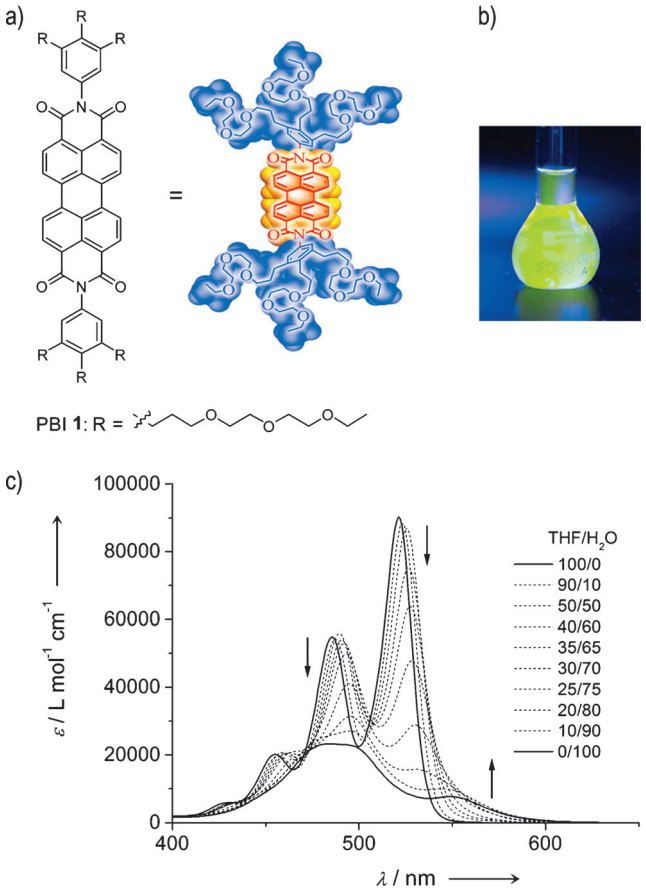

Figure 1. a) Chemical structure of PBI **1** and its space-filling (CPK) model. b) Photograph of a THF solution of PBI **1** (2.0×10^{-6} M) under a UV lamp. c) UV/Vis spectra of 2.0×10^{-6} M PBI **1** in THF/water mixtures at 20 °C. Arrows indicate spectral changes upon increase of water content.

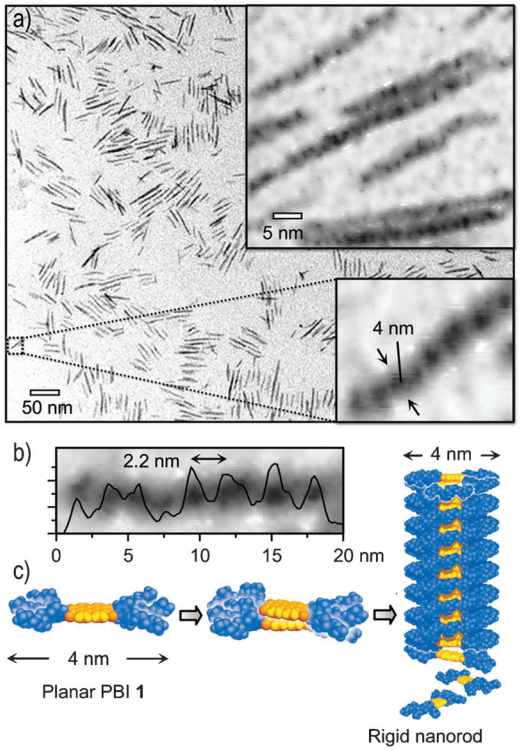

Figure 2. a) TEM images of segmented nanorods from PBI **1** aggregates in water, [PBI **1**] = 0.077 mg mL^{-1}. Inset: magnified TEM images showing segmented nanostructures. b) Electron density (relative darkness) curve of the cross-section along one nanorod. c) Schematic space-filling models illustrating the self-assembly of PBI **1**.

2.2 nm between two segments (Figure 2b). According to previously reported spectroscopic results and theoretical calculations, the rotational offset between two neighboring PBI molecules in a columnar π stack is 30°.[24] Therefore, six molecules should form a half turn (180°) and constitute one repeat unit, that is, a segment with a length of 2.2 nm as observed by TEM. Thus, the cofacial distance of two molecules is 0.36 nm (3.66 Å). This is the first time that the π–π stacking distance has been obtained by TEM experiments through real-space analysis.

An interesting hierarchical growth was observed for planar PBI **1**, when the preparation concentration is gradually increased in water (Figure 3). At an increased concentration of 0.25 mg mL^{-1} (ca. 0.16 mM), these nanorods begin to merge in a "side-to-side" manner into thicker nanostructures, and "side-to-side" division leads to thinner nanostructures; in other words, fusion and fission processes are in effect, as observed by TEM (Figure 3a,d) and confirmed by dynamic light scattering (DLS), cryogenic scanning electron microscopy (cryo-SEM), and atomic force microscopy (AFM) studies (for details, see the Supporting Information). The "side-to-side" fusion and fission process can be observed not only between two nanorods, but also for three and more nanorods (Figure 3d).

All these intermediate morphologies of nanorod fusion and fission can be observed at the same sample concentration in water, suggesting that the nanorod fusion and fission process is reversible. At a further increased sample concentration of 0.76 mg mL^{-1} (ca. 0.48 mM) and 1.0 mg mL^{-1} (ca. 0.63 mM) in water, these nanorods were fused together into single-molecule-layered nanoribbons with a width of 20–60 nm (Figure 3b,c). We point out that at this high concentration the TEM substrates were densely covered, leading now to a negative contrast, that is, a bright specimen, because the staining agent apparently does not penetrate into the densely packed supramolecular structure.[25] We attribute the different staining effect of the uranyl acetate contrast agent on the nanorod (positive staining) and nanoribbon (negative staining) specimens to the more open architecture of the former and the more closed structure of the latter. Cryo-SEM images taken at an intermediate concentration of PBI **1** (c = 0.25 mg mL^{-1}) showed a film consisting of interconnected thin nanorods (Figure S8) which could, however, not be resolved at the same level as that achieved by TEM with staining. The smallest resolved fibers had a width of (7.0 ± 2.0) nm. The cryo-SEM images of the more concentrated samples (c = 1.0 mg mL^{-1}) revealed the formation of a dense network (Figure S9) with nanoribbon widths of 30 to 300 nm. AFM measurements for films drop-casted from the same sample (1.0 mg mL^{-1}) on mica also disclosed nanoribbon structures

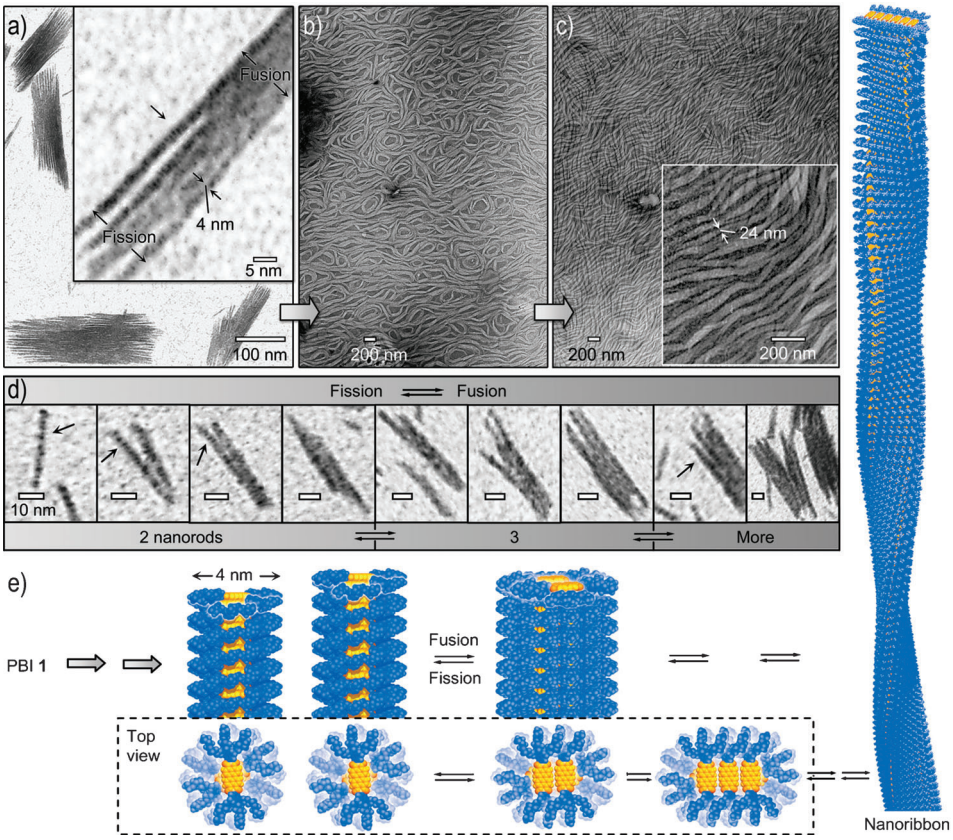

Figure 3. a–c) TEM images of PBI **1** aggregates prepared from water, [PBI **1**] = 0.25 mg mL^{-1} (a), 0.76 mg mL^{-1} (b), and 1.0 mg mL^{-1} (c). d) TEM images of the fusion and fission of two, three, or more nanorods; arrows indicate the segmented nanostructures, [PBI **1**] = 0.25 mg mL^{-1}; scale bar: 10 nm. e) Schematic illustration based on space-filling (CPK) models for the hierarchical self-assembly from nanorods to nanoribbons by fusion and fission.

(Figure 4). Cross-section analysis of these structures reveal a height of about 4 nm in accordance with the length of PBI **1** and nanoribbon widths of 20–60 nm (Figure 4, inset).[26]

The fact that the hydrophobic scaffolds of the original PBI nanorods are, according to our molecular modelling, not entirely buried in the aqueous environment is thought to be the driving force for the formation of nanoribbons at higher concentration where the whole hydrophobic core is enwrapped by the OEG chains (Figure 3e). It is interesting that the fusion of two helical PBI columns with side-by-side organization of PBIs has been reported recently for a structurally very similar molecule in the solid-state by Percec and coworkers based on XRD and solid-state NMR investigations.[27] These authors as well as Yagai et al.[28] furthermore described the subtle balance between columnar and lamellar liquid-crystalline phases for this class of dyes.[29] What distinguishes our work from these previous studies is the direct visualization of the hierarchical growth process in a solvent environment which was possible due to the ultrastrong PBI–PBI stacking forces in water.

Like PBI micelles[30] and vesicles[17,31] these water-dissolved columnar PBI dye aggregates are light-emitting in the red and near-infrared region from 500 nm up to 850 nm under ultraviolet or visible-light irradiation (Figure 5). The pronounced red-shift and broadening of the emission band is characteristic for closely cofacially stacked planar PBIs and has been attributed to a structural relaxation process of excited PBI aggregates, leading to a localization of the excitation energy on an excimer unit.[24] Most interestingly, for PBI **1** aggregates the fluorescence intensity increases considerably with the hierarchical growth from nanorods (fluorescence quantum yield Φ_F = 1.7%) to nanoribbons (Φ_F = 6.8%). At the same time the fluorescence lifetime changes from a bi-exponential decay (main component 11 ns) for concentrations up to 0.1 mg mL^{-1} to a mono-exponential decay with a longer lifetime of 20 ns (for details see Table S1 in the Supporting Information). These observations are in contradiction to the common perception that fluorescence quantum yields (and concomitantly lifetimes) decrease with increasing concentration due to self-quenching, reabsorption, and other fluorescence-quenching processes;[32] however, also the opposite, that is, aggregation-induced emission (AIE), has been reported for a number of dyes more recently.[33] Despite the significant interest in this field, to the best of our knowledge an AIE effect has never been traced back to the specific supramolecular reorganization of dye molecules, as given here upon hierarchical growth

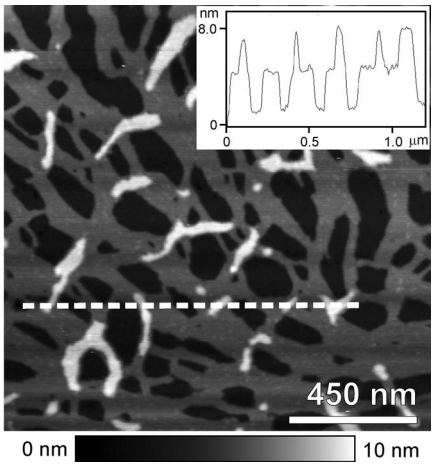

Figure 4. AFM image of nanoribbons of PBI **1** aggregates deposited from water, [PBI **1**] = 1.0 mg mL^{-1}. Inset: cross-section analysis along the dotted line.

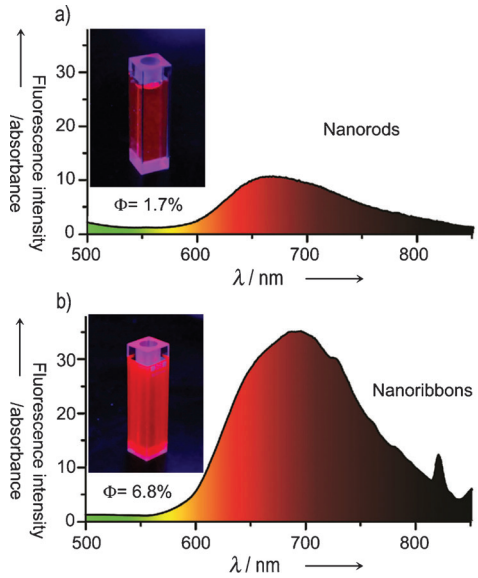

Figure 5. Photoluminescence properties of perylene dye aggregates in water. a) Fluorescence spectrum of nanorods in water, [PBI **1**] = 0.077 mg mL^{-1}. b) Fluorescence spectrum of nanoribbons in water, [PBI **1**] = 1.0 mg mL^{-1}. Insets in (a) and (b): photograph of the respective aggregate solutions under an ultraviolet lamp. Fluorescence quantum yields (Φ) are indicated. Fluorescence spectra were corrected for absorption.

from nanorods to nanoribbons. Because this reorganization is not accompanied by obvious changes in the UV/Vis spectra (like that seen, for example, for the transformation from H- to J-aggregates) the most likely explanation is that the more dense packing arrangement of the PBI molecules in the nanoribbons disfavors structural relaxation pathways in the excited state that are known to afford less fluorescent aggregates for this class of dyes.[24,34]

In conclusion, we have observed the sequential self-assembly of PBI **1** dyes from nanorods to nanoribbons upon increasing concentration in water by TEM and UV/Vis, DLS, cryo-SEM, and AFM analysis. Concomitant with the fusion of nanorods to nanoribbons, a pronounced increase in fluorescence quantum yields was observed, which is attributed to the denser packing of the dyes which disfavors the structural relaxation into less fluorescent excimer species. Our elucidation of PBI assembly from the molecular level to small and large supramolecular nanosystems constitutes a bridge between molecules and their morphologies and functions, and thus provides a guideline for the design of advanced molecular materials.

Received: October 14, 2013
Published online: December 18, 2013

Keywords: aggregates · amphiphiles · dyes/pigments · fluorescence · nanostructures

[1] M. A. Quadir, R. Haag, *J. Controlled Release* **2012**, *161*, 484–495.
[2] S. Matile, A. V. Jentzsch, A. Fin, J. Montenegro, *Chem. Soc. Rev.* **2011**, *40*, 2453–2474.
[3] a) D. González-Rodríguez, J. L. van Dongen, M. Lutz, A. L. Spek, A. P. H. J. Schenning, E. W. Meijer, *Nat. Chem.* **2009**, *1*, 151–155; b) V. Percec, A. E. Dulcey, V. S. K. Balagurusamy, Y. Miura, J. Smidrkal, M. Peterca, S. Nummelin, U. Edlund, S. D. Hudson, P. A. Heiney, H. Duan, S. N. Magonov, S. A. Vinogradov, *Nature* **2004**, *430*, 764–768.
[4] A. Falanga, M. Cantisani, C. Pedone, S. Galdiero, *Protein Pept. Lett.* **2009**, *16*, 751–759.
[5] H. Ringsdorf, B. Schlarb, J. Venzmer, *Angew. Chem.* **1988**, *100*, 117–162; *Angew. Chem. Int. Ed. Engl.* **1988**, *27*, 113–158.
[6] J. A. A. W. Elemans, A. E. Rowan, R. J. M. Nolte, *J. Mater. Chem.* **2003**, *13*, 2661–2670.
[7] X. Zhang, C. Wang, *Chem. Soc. Rev.* **2011**, *40*, 94–101.
[8] H. J. Kim, T. Kim, M. Lee, *Acc. Chem. Res.* **2011**, *44*, 72–82.
[9] T. Aida, E. W. Meijer, S. I. Stupp, *Science* **2012**, *335*, 813–817.
[10] X. Zhang, Z. Chen, F. Würthner, *J. Am. Chem. Soc.* **2007**, *129*, 4886–4887.
[11] V. Percec, D. A. Wilson, P. Leowanawat, C. J. Wilson, A. D. Hughes, M. S. Kaucher, D. A. Hammer, D. H. Levine, A. J. Kim, F. S. Bates, K. P. Davis, T. P. Lodge, M. L. Klein, R. H. DeVane, E. Aqad, B. M. Rosen, A. O. Argintaru, M. J. Sienkowska, K. Rissanen, S. Nummelin, J. Ropponen, *Science* **2010**, *328*, 1009–1014.
[12] M. J. Mayoral Muñoz, G. Fernández, *Chem. Sci.* **2012**, *3*, 1395–1398.
[13] E. Krieg, H. Weissman, E. Shirman, E. Shimoni, B. Rybtchinski, *Nat. Nanotechnol.* **2011**, *6*, 141–146.
[14] A. Ajayaghosh, R. Varghese, S. Mahesh, V. K. Praveen, *Angew. Chem.* **2006**, *118*, 7893–7896; *Angew. Chem. Int. Ed.* **2006**, *45*, 7729–7732.
[15] Z. Huang, S.-K. Kang, M. Banno, T. Yamaguchi, D. Lee, C. Seok, E. Yashima, M. Lee, *Science* **2012**, *337*, 1521–1526.
[16] S. Yagai, M. Yamauchi, A. Kobayashi, T. Karatsu, A. Kitamura, T. Ohba, Y. Kikkawa, *J. Am. Chem. Soc.* **2012**, *134*, 18205–18208.
[17] D. Görl, X. Zhang, F. Würthner, *Angew. Chem.* **2012**, *124*, 6434–6455; *Angew. Chem. Int. Ed.* **2012**, *51*, 6328–6348.
[18] C. Backes, F. Hauke, A. Hirsch, *Adv. Mater.* **2011**, *23*, 2588–2601.
[19] Z. Chen, A. Lohr, C. R. Saha-Möller, F. Würthner, *Chem. Soc. Rev.* **2009**, *38*, 564–584.
[20] a) Z. Chen, B. Fimmel, F. Würthner, *Org. Biomol. Chem.* **2012**, *10*, 5845–5855; b) Z. Chen, V. Stepanenko, V. Dehm, P. Prins, L. D. A. Siebbeles, J. Seibt, P. Marquetand, V. Engel, F. Würthner, *Chem. Eur. J.* **2007**, *13*, 436–449.
[21] B. Rybtchinski, *ACS Nano* **2011**, *5*, 6791–6818.
[22] We note that for the vast majority of one-dimensional dye aggregates formed by isodesmic supramolecular polymerization only very small-sized aggregates are formed in organic solvents.
[23] Since positive staining involves the direct coordination of the contrasting agent (uranyl acetate) to the investigated specimen, we cannot exclude the possibility of concomitant structural rearrangement. Because of the perfect agreement between the model for the columnar packing derived from TEM and previous spectroscopic results on related dye aggregates, this type of rearrangement should not be very pronounced.
[24] R. F. Fink, J. Seibt, V. Engel, M. Renz, M. Kaupp, S. Lochbrunner, H.-M. Zhao, J. Pfister, F. Würthner, B. Engels, *J. Am. Chem. Soc.* **2008**, *130*, 12858–12859.
[25] In TEM analysis of biological samples negative staining is always preferred because it does not lead to structural changes of the investigated specimen; see Ref. [23].
[26] We point out that the use of mica as the substrate supports the adsorption of rather hydrophilic structures on the surface. Usually this does not influence the morphology of aggregates.

[27] V. Percec, M. Peterca, T. Tadjiev, X. Zeng, G. Ungar, P. Leowanawat, E. Aqad, M. R. Imam, B. M. Rosen, U. Akbey, R. Graf, S. Sekharan, D. Sebastiani, H. W. Spiess, P. A. Heiney, S. D. Hudson, *J. Am. Chem. Soc.* **2011**, *133*, 12197 – 12219.
[28] S. Yagai, M. Usui, T. Seki, H. Murayama, Y. Kikkawa, S. Uemura, T. Karatsu, A. Kitamura, A. Asano, S. Seki, *J. Am. Chem. Soc.* **2012**, *134*, 7983 – 7994.
[29] Another model for the formation of lamellar structures from columnar self-assemblies has recently been proposed for sugar-bearing perylene bisimide amphiphiles: J. Hu, W. Kuang, K. Deng, W. Zou, Y. Huang, Z. Wei, C. F. J. Faul, *Adv. Funct. Mater.* **2012**, *22*, 4149 – 4158.
[30] X. Zhang, D. Görl, F. Würthner, *Chem. Commun.* **2013**, *49*, 8178 – 8180.
[31] X. Zhang, S. Rehm, M. M. Safont-Sempere, F. Würthner, *Nat. Chem.* **2009**, *1*, 623 – 629.
[32] J. R. Lakowicz, *Principles of Fluorescence Spectroscopy*, Plenum, New York, **1999**.
[33] Y. Hong, J. W. Y. Lam, B. Z. Tang, *Chem. Soc. Rev.* **2011**, *40*, 5361 – 5388.
[34] H. Yoo, J. Yang, A. Yousef, M. R. Wasielewski, D. Kim, *J. Am. Chem. Soc.* **2010**, *132*, 3939 – 3944.

